Applied Environmental Research (2027) 49(1), 004
https://doi.org/10.35762/AER.2027004

Applied Environmental Research
- RESEARCH FOR SUSTAINABLE PLANET -



Research Article

Efficient Removal of Tannins from Vinasse with Citric Acid-Modified Sugarcane Bagasse: Process Optimization Via Response Surface Methodology, Kinetic and Equilibrium Studies

Nicomedes Ariel Jaramillo-González[1], Mónica Miranda[2], Jorge Ceballos[3], Rosa Elena Caballero[2,*]

[1] Programa de Maestría en Investigación, Vicerrectoría de Investigación y Posgrado, Universidad Autónoma de Chiriquí, Chiriquí, Panamá
[2] Centro Especializado en Investigaciones de Química Inorgánica y Afines, Facultad de Ciencias Naturales y Exactas, Universidad Autónoma de Chiriquí, Chiriquí, Panamá
[3] Laboratorio de Biociencias, Biotecnología y Ciencias Aplicadas, Facultad de Ciencia y Tecnología, Universidad Tecnológica de Panamá, Panamá, Panamá

*Corresponding Email: rosa.caballero@unachi.ac.pa

Abstract

This study evaluated the efficiency of tannin removal from vinasse using sugarcane bagasse as a biosorbent before and after citric acid modification. A central composite design optimized the modification process, considering bagasse mass, citric acid concentration, and reaction time as independent variables. The FTIR intensity ratio at 1,730/3,400 cm^{-1} (I1730/I3400) was the response variable, where an increase indicated greater carbonyl incorporation, with 1,730 and 3,400 cm^{-1} assigned to C=O and O–H stretching, respectively. We optimized the biosorption conditions using the same statistical design, with pH, bagasse mass, and vinasse concentration as the factors and tannin removal efficiency as the response. Both raw and modified bagasse samples were characterized by FTIR, SEM, pHpzc, and surface functional group analysis; the spent adsorbent was analyzed by FTIR and confocal microscopy. Optimal modification was achieved with 10% w/v citric acid, 1.0 g bagasse, and a 20-minute reaction, yielding an FTIR I1730/I3400 ratio of 1.458, indicating successful esterification. The optimal biosorption contact time was set at 120 minutes based on kinetic data showing rapid adsorption during the initial 30 minutes. Under these conditions, citric acid-modified bagasse outperformed raw bagasse in terms of both removal efficiency and pH independence. The kinetic data conformed to a pseudo-second-order model, indicating that intraparticle diffusion was not the sole adsorption mechanism. The equilibrium data fit the Freundlich isotherm, and the experimental adsorption capacity reached 64.84 mg g^{-1} under optimal conditions. Evidence suggests that tannin adsorption onto citric acid-modified bagasse occurs via a mixed mechanism involving both physical and specific surface interactions. Confocal microscopy confirmed the presence of phenolic compounds on the bagasse surface. These results highlight the potential of citric acid-modified bagasse for treating tannin-rich effluents. Further research should address surface area, regeneration, and performance of diverse adsorbates to fully realize the potential of these sustainable materials.

ARTICLE HISTORY

Received: 9 Feb. 2026
Revised: 22 Sep. 2026
Accepted: 1 Oct. 2026
Published: 22 Oct. 2026

KEYWORDS

Effluents;
Functional groups;
Lignocellulosic materials;
Value-added products

Introduction

The sugarcane industry generates large quantities of lignocellulosic residues, among which bagasse is among the most abundant. This residue, produced during sugarcane pressing for juice extraction, accounts for approximately 25% to 29% of the total processed biomass (Jacome-Pilco et al., 2023). In Panama, more than 2 million tons of sugarcane were harvested during the 2022–2023 period; therefore, bagasse accumulation represents a significant environmental challenge (Ministerio de Desarrollo Agropecuario, 2023). Although this byproduct has several applications in other contexts, its reported use in Panama is mainly limited to energy generation within the sugarcane industry. Moreover, some studies have documented its potential as a construction material (Cascaret-Carmenaty et al., 2020; Chingono et al., 2018; Chumpiboon et al., 2022; Jacome-Pilco et al., 2023; Marin et al., 2021; Ungureanu et al., 2022).

The production of ethanol from sugarcane generates substantial quantities of vinasse, a byproduct with a high contaminant load, typically 10–20 liters per liter of distilled ethanol (Silva et al., 2021). Vinasse is rich in recalcitrant organic compounds, such as melanoidins, organic acids, and phenolic compounds, which present significant challenges for management, treatment, and valorization (Caputo, 2020; Jacome-Pilco et al., 2023; Kee et al., 2023; Montiel-Rosales et al., 2022). Among these compounds, phenolic compounds are of particular concern because of their toxicity, environmental persistence, potential for bioaccumulation, and well-documented mutagenic and carcinogenic effects in aquatic ecosystems (Anku et al., 2017; Othmani et al., 2022).

Reported uses of vinasse include fertigation, energy production, biogas generation, animal-feed production, and use as a raw material in biological treatments, including the production of soil enhancers (Jacome-Pilco et al., 2023; Kee et al., 2023; Reis and Hu, 2017; Rulli et al., 2021; Solano et al., 2020). To our knowledge, no well-established policies currently regulate vinasse valorization or treatment in Panama. Nonetheless, academic research has investigated the biotreatment of vinasse using white rot fungi (Caballero et al., 2024).

Several studies have documented the use of sugarcane bagasse as a biosorbent. For example, de Aquino Lima et al. (2024) evaluated the direct use of sugarcane bagasse and peanut shells as natural biosorbents for vinasse treatment, achieving partial reductions in organic matter and turbidity. Siqueira et al. (2020) evaluated the kinetics, thermodynamics, and adsorption models associated with the use of sugarcane bagasse as a biosorbent for methylene blue removal.

The potential of lignocellulosic materials as biosorbents for contaminant removal in aqueous media represents an economically and environmentally sustainable alternative to conventional synthetic materials (Dai et al., 2018; Othmani et al., 2022; Torres, 2020; Tyagi and Anand, 2024). Owing to their high cellulose, hemicellulose, and lignin contents, these materials provide a porous, functionalized structure that can be exploited in biosorption processes (Ajala et al., 2021; Gomes et al., 2020; Kerrou et al., 2021; Mpatani et al., 2021). However, the biosorption efficiency of sugarcane bagasse and other lignocellulosic residues can be improved through modifications that increase their application in the removal of various contaminants (Yadav et al., 2021). These findings confirm the potential of bagasse as a starting material for more advanced remediation strategies.

Esterification of sugarcane bagasse with citric acid has been proposed as a low-cost and environmentally friendly approach to enhance biomass functionalization. Recent studies have shown that this modification increases the availability of carboxyl groups on the bagasse surface, promoting interactions with phenolic compounds (Gomes et al., 2020). Citric acid-modified bagasse has also been reported to achieve adsorption capacities above 230 mg g^{-1} for model dyes such as methylene blue, exhibit pseudo-second-order kinetics, fit a Freundlich isotherm, and maintain high regeneration efficiency after multiple use cycles (Mpatani et al., 2020).

However, the application of this strategy to vinasse, a high-strength effluent generated by the sugarcane industry, has rarely been reported. Moreover, studies that simultaneously optimize the modification process and biosorption performance while validating the resulting structural changes remain limited.

In Panama, one of the main industries depends on crops such as sugarcane (Atencio et al., 2020). Valorizing bagasse would not only reduce its accumulation but also promote the implementation of clean technologies aligned with circular-economy principles. Therefore, generating baseline information is relevant for supporting the development of methods that can shorten production cycles and minimize environmental impacts.

In this context, the present study aimed to evaluate the tannin-removal capacity of vinasse using citric acid-esterified sugarcane bagasse. We used a response surface design to optimize both the modification and biosorption processes; analyzed the influential variables; and explored structural and morphological changes via infrared spectroscopy (FTIR), scanning electron microscopy (SEM), confocal microscopy, point of zero charge (pH_{PZC}), and determination of surface acidic and basic groups. We also studied the adsorption kinetics and isotherms.

Materials and methods

1) Collection and preparation of the adsorbent material

We collected 15 kg of sugarcane bagasse as a byproduct of artisanal juice extraction. The bagasse was washed thoroughly with water and air-dried for 5

days, then milled and sieved using an ASTM 500 µm mesh and stored in plastic bags with silica gel to control moisture. The raw material was coded as BC1.

To obtain modified bagasse (BC2), an esterification procedure adapted from Mpatani et al. (2020) was used. The treatment consisted of mixing the bagasse with aqueous citric acid solutions, followed by a thermal protocol that included sonication in a VWR B2500A-MTH ultrasonic bath for 30 minutes and subsequent heating at approximately 100 °C for 10 to 70 minutes. After treatment, the material was filtered, dried in an Across International StableTemp-25 oven at 45 °C for 48 hours, and stored in airtight bags with silica gel (Jaramillo-González, 2025).

2) Optimization of the citric acid modification process

A central composite design (CCD) with five levels (-α, -1, 0, +1, +α) was utilized to evaluate the effects of three variables: bagasse mass (A; 0.25–1.75 g), citric acid concentration (B; 0–12% w/v), and reaction time (C; 10–70 minutes). The response variable was the spectral intensity ratio I1730/I3400 obtained by Fourier transform infrared spectroscopy (FTIR), where I1730 and I3400 were defined as the maximum absorbance values of the bands near 1,730 and 3,400 cm^{-1}, respectively (Jaramillo-González, 2025). We determined the absorbance values directly from the acquired spectra without postacquisition normalization. For each spectrum, the local maximum of each band was selected to account for small shifts in band position among samples. Spectra were obtained using a Shimadzu IRAffinity-1S spectrometer (Shimadzu Corp., Japan) coupled to a MIRacle™ Single Reflection attenuated total reflectance (ATR) accessory (PIKE Technologies, USA) equipped with a zinc selenide (ZnSe) crystal. The band at 1,730 cm^{-1} corresponds to the stretching of carbonyl groups (C=O) associated with ester and carboxyl functiona-lities, whereas the band at 3,400 cm^{-1} is attributed to the stretching of hydroxyl groups (O–H) present in cellulose and hemicellulose (Mpatani et al., 2020; Zara et al., 2017). We used the I1730/I3400 ratio as an indicator of esterification, with a relative increase in the 1,730 cm^{-1} signal relative to the 3,400 cm^{-1} band reflecting greater conversion of hydroxyl groups to ester groups after citric acid treatment (Aruna et al., 2021; Hoang et al., 2021; Ly et al., 2018; Santos et al., 2012).

3) Bagasse characterization

We analyzed BC1, BC2, and spent adsorbent using FTIR. Confocal microscopy was applied to the residual bagasse after biosorption (Jaramillo-González, 2025). The point of zero charge (pHpzc), surface acidic and basic groups, and surface morphology were investigated for BC1 and BC2.

3.1) Infrared spectroscopy (FTIR)

Spectra were obtained using a Shimadzu IRAffinity-1S spectrometer (Shimadzu Corp., Japan) coupled to a MIRacle™ Single Reflection ATR accessory with a ZnSe crystal (PIKE Technologies, USA) in the range of 4,000–400 cm^{-1}, with a resolution of 4 cm^{-1} and 40 scans.

3.2) Scanning electron microscopy (SEM)

The morphology of the samples was evaluated using a Thermo Fisher Scientific Quattro S scanning electron microscope (FEG-SEM, Thermo Fisher Scientific, USA) operated in low-vacuum mode at 10.0 kV and a working distance of 10.8 mm.

3.3) Confocal microscopy

Fluorescence analysis was performed using an Olympus Fluoview FV3000 confocal microscope (Olympus Corp., Japan) with excitation lasers at 405, 488, and 561 nm and a 4× objective in spectral mode. This analysis explored the natural autofluorescence of bagasse and revealed possible variations in its interactions with phenolic compounds. During image acquisition, parameters such as laser transmissivity and AOTF/AOM settings, PMT voltage, and detection ranges (DAPI: 430–470 nm; SD1 green: 500–600 nm; and SD2 red: 570–620 nm) were controlled to ensure comparability across the experimental conditions of the different samples (spents BC1 and BC2).

3.4) Point of zero charge (pHpzc)

The pH at the point of zero charge was determined according to the methods of Bakatula et al. (2018) and Crespão et al. (2021) with some modifications. In 250 mL Erlenmeyer flasks, 0.4 g of the sample was added to 40.0 mL of 0.1 M KCl solution. The pH was adjusted with 0.1 M HCl and 0.1 M NaOH to achieve a pH range of 2–10 (± 0.1 pH units). The pH of the supernatant was recorded as the initial pH (pHi). The samples were shaken for 48 hours at 150 rpm. After settling, the final pH (pHf) of the supernatant in each flask was measured. The point of zero charge (pHpzc) was determined by plotting ΔpH (pHf – pHi) against pHi.

3.5) Surface acid and basic groups

Surface functional groups were characterized following the Boehm methodology, as described by Schönherr et al. (2018). To determine the total acidic groups, 0.5 grams of adsorbent was mixed with 50 mL of 0.1 M standard solution of sodium hydroxide (NaOH) in a 250 mL Erlenmeyer flask. The flasks were sealed and agitated in a shaker at 30 °C and 150 rpm for 24 hours. The suspensions were filtered (0.7 µm microfibers), and a 10 mL aliquot was titrated with 0.1 M hydrochloric acid (HCl) standard solution. To determine basic groups, 0.5 g of bagasse was suspended in 50 mL of 0.1 M

hydrochloric acid under the conditions described above. A 10 mL aliquot was titrated with 0.1 M sodium hydroxide under continuous stirring. The functional groups identified in the residues were calculated as mmol g^{-1}. All the samples were analyzed in triplicate.

4) Vinasse samples

A 30 L vinasse sample was collected at a local distillery directly from the outlet line before it was mixed with other effluents. The samples were stored in opaque containers at 7 °C. Before use, they were allowed to equilibrate to room temperature, homogenized by agitation, and centrifuged in a Hermle Benchmark Z287-A centrifuge at 6000 rpm for 10 minutes. Dilutions (% v/v) were prepared from the supernatant.

Vinasse characterization included the following parameters: pH, COD (mg L^{-1}), total solids (mg L^{-1}), conductivity (µS cm^{-1}), turbidity (NTU), color (mg L^{-1}), and total tannins (mg L^{-1}). Analyses were performed following standard methods (APHA/AWWA/WEF, 2017).

5) Biosorption assays

5.1) Evaluation of contact time

Contact times ranging from 30 to 210 minutes were evaluated for BC1 and BC2, using 0.4 g of adsorbent and vinasse at 15% and 55% (v/v) (Chumpiboon et al., 2022; Kerrou et al., 2021). The tests were conducted in 250 mL reactors, with 3 replicates per treatment and a total working volume of 40 mL, under orbital agitation at 150 rpm and room temperature (26–28 °C). The total tannin concentration, expressed in mg L^{-1}, was determined before and after treatment using the official AOAC 952.03 method (AOAC, 2005). The removal efficiency (%), as shown in Eq. 1, was calculated from the initial and final tannin concentrations (Jaramillo-González, 2025).

$$R\% = [C_o - C_f]/C_0 \times 100 \qquad \text{(Eq.1)}$$

where Co and Cf are the initial and final tannin concentrations, respectively.

5.2) Optimization of biosorption conditions

A CCD with three levels (-1, 0, +1) was applied for each biosorbent (BC1 and BC2). The evaluated variables were pH (A; 3–7), bagasse dosage (B; 0.20–0.40 g), and vinasse dilution (C; 50–100% v/v). The temperature was fixed at 30 °C using a Shel Lab – SLI – Sheldon shaker (Sheldon, USA) operating at 150 rpm. The response variable was the removal efficiency (%), which was calculated from the initial and final total tannin concentrations (mg L^{-1}) (Jaramillo-González, 2025).

6) Equilibrium and kinetic studies

Batch equilibrium studies apply empirical models to describe adsorption behavior. Here, we use the Langmuir, Freundlich, and Temkin isotherm models, which are widely recognized (Samuel et al., 2020). The experiments were conducted as follows: 250 mL Erlenmeyer flasks at 150 rpm, 0.1 g of adsorbent, a reaction volume of 20 mL, vinasse concentrations (%v/v) of 10, 20, 30, 40, and 50%, and working temperatures of 30, 35, and 40 °C. The optimal conditions (pH = 3 and contact time = 120 minutes) were applied. All experiments were carried out in triplicate.

Various models have been applied to describe the kinetic behavior of adsorption systems. In this study, we used pseudo-first-order, pseudo-second-order, and intraparticle diffusion models after time-dependent data were collected (Mpatani et al., 2020). The response variables in the equilibrium and kinetic studies were defined by the following Eqs. 2–4:

$$q_e = V(C_o - C_e)/m \qquad \text{(Eq. 2)}$$

$$q_t = q_e\left(1 - e^{-k_1 t}\right) \qquad \text{(Eq. 3)}$$

$$q_t = k_2 q_e^2 t/(1 + k_2 q_e t) \qquad \text{(Eq. 4)}$$

where q_e is the equilibrium adsorption capacity (mg g^{-1}); q_t is the adsorption capacity at time t (mg g^{-1}); C_o and C_e are the initial and equilibrium concentrations of the adsorbate in the liquid phase, respectively (mg L^{-1}); *V* is the volume of the adsorbate solution (L); m is the mass of adsorbent used (g); t is the adsorption time (min); k_1 is the pseudo-first-order rate constant (min^{-1}); and k_2 is the pseudo-second-order rate constant (g mg^{-1} min^{-1}).

7) Statistical analysis

For the kinetic data (contact time), normality was verified using the Shapiro–Wilk test ($p > 0.05$). When this assumption was met, we applied ANOVA followed by Tukey's HSD test ($p < 0.05$) for mean comparisons using the online platform StatsKingdom (https://www.statskingdom.com/). For the optimization experiments, Design-Expert v13.0.5.0 (Stat-Ease Inc., USA) was used for the experimental design and data analysis.

Results and discussion

1) Optimization of the citric acid modification process

Esterification with citric acid resulted in I1730/ I3400 ratios ranging from 0.302 to 1.602 (Table 1). In the central composite design, factor A represented the mass of bagasse (g), factor B represented the citric acid concentration (% w/v), and factor C represented the reaction time (min). Higher values were observed

for higher citric acid concentrations (up to 10% w/v) and shorter reaction times (20 minutes).

The spectra obtained from the 24 experiments are shown in Figure 1. Variations in the intensity of several signals across the spectral range reflect changes in the material's response under different experimental conditions. However, the spectra maintain the same general band pattern, suggesting that the chemical modification of sugarcane bagasse occurred consistently (Jaramillo-González, 2025).

More specifically, the relative decrease in the signal at 3400 cm^{-1} (O–H stretching) and the increase in the band at 1730 cm^{-1} (C=O stretching of esters and free carboxyl groups) are confirmed by the I1730/I 3400 values shown in Table 1. This trend suggests that the hydroxyl groups convert to ester bonds during the citric acid treatment. Mpatani et al. (2020) reported similar results. They reported reduced O–H band intensity and an increased C=O peak in citric acid-modified bagasse during methylene blue removal from aqueous solutions.

In their study, they interpreted these bands qualitatively to confirm chemical modification, while the design of experiments (DOE) optimization focused on the dye adsorption stage by evaluating variables such as the pH, biosorbent dosage, and dye concen-tration. In contrast, in the present work, both the modification process and the biosorption experiments were optimized.

Equation 5 represents the reduced quadratic model in coded units with a variable transformation for the citric acid-modified sugarcane bagasse. The analysis of variance (ANOVA) results revealed that the model is highly significant ($F = 63.92$, $p < 0.0001$), suggesting a strong relationship between the variables. The lack-of-fit F value of 0.59 is not statistically significant compared with the pure error ($p = 0.7763$). Overall, the model showed a good fit, with $R^2 = 0.9523$, adjusted $R^2 = 0.9374$, predicted $R^2 = 0.9058$, and an adequate precision of 30.25, suggesting reliable predictive capability (Jaramillo-González, 2025).

Strong agreement between the predicted and observed values for the transformed variable 1/(I1730/I3400) is shown in Figure 2a. The dispersion around the diagonal line is minimal and appears random, indicating that the model effectively captures the principal trends within the data. These findings support the validity of the model for prediction and factor analysis across the experimental range studied. The model with the 1/(I1730/I3400) transformation reasonably satisfies the assumption of residual normality. No severe outliers or systematic patterns were identified that would indicate significant violations of the normality assumption (Figure 2b).

$$1/\mathrm{I1730/I3400} = 1.79 - 0.7729\mathrm{B} - 0.1049\mathrm{C} + 0.2187\mathrm{BC} + 0.2611\mathrm{B}^2 - 0.4325\mathrm{C}^2 \quad \text{(Eq. 5)}$$

Table 1 CCD matrix for the modification of bagasse with citric acid

Run	Factors			I1730 cm^{-1}	I3400 cm^{-1}	I1730/I3400	
	A	B	C	Abs	Abs	Experimental	Prediction
1	1.50	2.0	20	0.029	0.086	0.337	0.369
2	0.25	6.0	40	0.05	0.095	0.526	0.559
3	0.50	2.0	20	0.025	0.067	0.373	0.369
4	0.50	2.0	60	0.022	0.047	0.468	0.485
5	1.00	6.0	40	0.109	0.193	0.565	0.559
6	1.75	6.0	40	0.101	0.176	0.574	0.559
7	1.00	6.0	70	0.205	0.128	1.602	1.524
8	1.00	12.0	40	0.021	0.027	0.778	0.826
9	1.00	6.0	40	0.085	0.148	0.574	0.559
10	1.00	6.0	40	0.078	0.146	0.534	0.559
11	1.00	6.0	40	0.071	0.144	0.493	0.559
12	1.00	0.0	40	0.019	0.063	0.302	0.283
13	1.00	6.0	40	0.113	0.182	0.621	0.559
14	1.00	6.0	40	0.036	0.085	0.424	1.046
15	1.50	10.0	60	0.092	0.101	0.911	0.485
16	1.50	2.0	60	0.046	0.099	0.465	0.559
17	1.00	6.0	40	0.131	0.189	0.693	1.030
18	1.00	6.0	10	0.104	0.089	1.169	0.559
19	1.00	6.0	40	0.054	0.111	0.486	1.372
20	1.00	6.0	40	0.108	0.125	0.864	0.559
21	1.50	10.0	20	0.085	0.057	1.491	1.372
22	1.00	6.0	40	0.039	0.065	0.600	1.046
23	0.50	10.0	20	0.053	0.042	1.262	0.369
24	0.50	10.0	60	0.066	0.050	1.320	0.559

Remark: Adapted from: Jaramillo-González (2025).

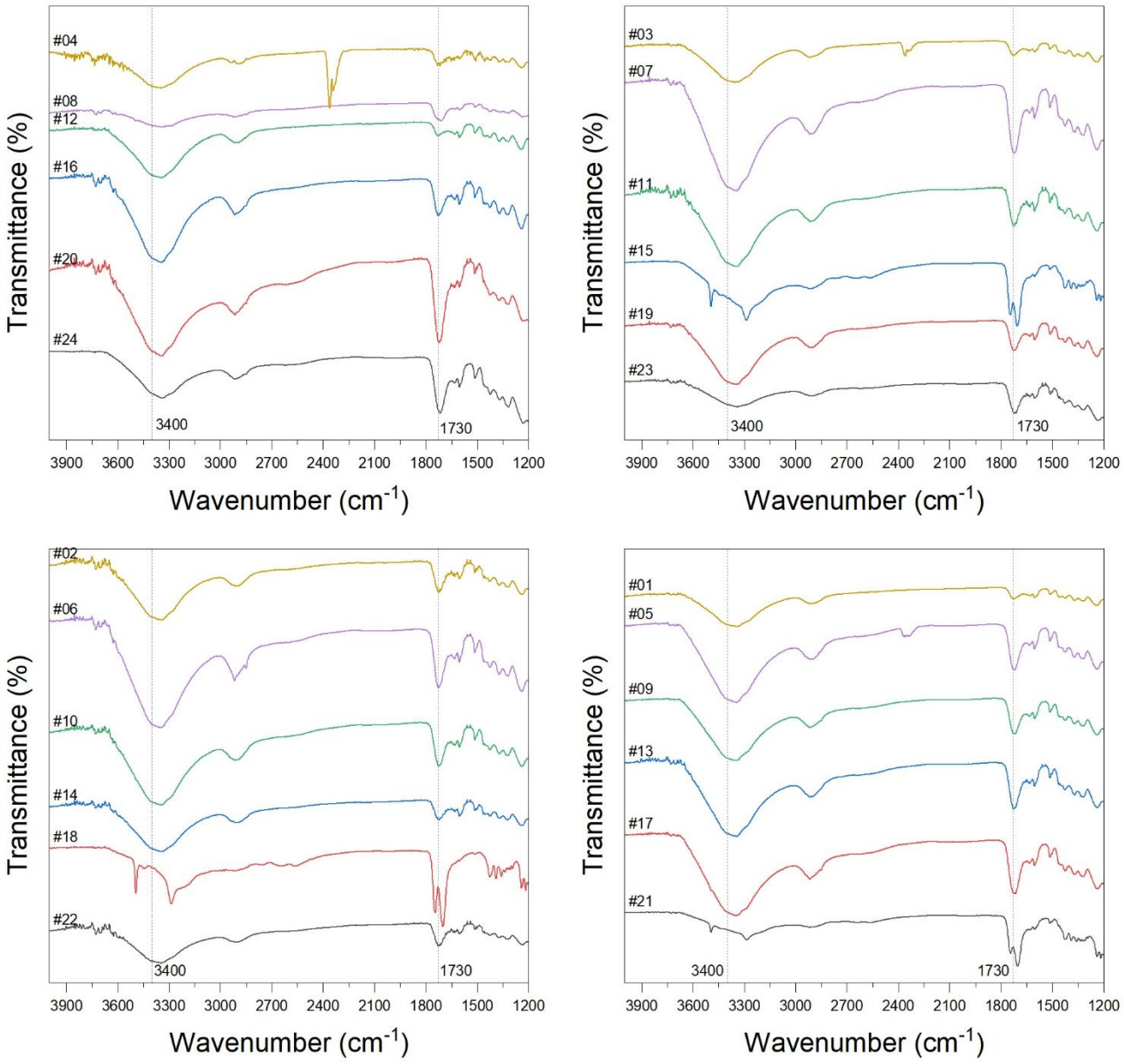


Figure 1 Infrared spectra of the bagasse modification experiments.

The linear effect of the citric acid concentration (B) was highly significant ($F = 225.18$; $p < 0.0001$), whereas the linear effect of the reaction time (C) was not significant ($p = 0.0585$). However, the quadratic effect of time (C^2) was marked ($F = 61.78$, $p < 0.0001$), as was the quadratic effect of the citric acid concentration (B^2) ($F = 22.52$, $p = 0.0002$). The interaction between B and C was also significant ($F = 11.54$, $p = 0.0037$). In contrast, the amount of bagasse (A) did not have a significant effect and was therefore excluded from the final model.

The response surface (Figure 3) shows that the I1730/I3400 ratio is maximized at short reaction times (20 minutes) and high citric acid concentrations, with the bagasse mass at its optimum. Numerical optimization at a desirability value of 0.961 revealed the following optimal conditions: 10.0% w/v citric acid, 1.0 g of bagasse, and 20 minutes of reaction time, with a predicted I1730/I3400 ratio of 1.458. On the basis of these graphical results, we recommend expanding the experimental range to determine whether a larger optimal response region exists.

In other sugarcane valorization studies, for example, the experiment by Gomes et al. (2020), citric acid was used as a pretreatment for sugarcane bagasse before enzymatic hydrolysis. They optimized the reaction time and citric acid concentration (% w/w) and treated lignin, cellulose, and hemicellulose as responses. In this experiment, longer reaction times resulted in higher yields of total reducing sugars, with no effect on the citric acid concentration.

2) Bagasse characterization

2.1) Infrared spectroscopy (FTIR)

The FTIR spectra of BC1 and BC2 showed characteristic changes (Figure 4). In BC1, the band at 3400 cm^{-1} corresponded to hydroxyl groups, whereas the signal at 1,730 cm^{-1} was associated with carbonyls

present in lignin. In BC2, these bands shifted to 3,281 cm^{-1} and 1,743 cm^{-1}, respectively, with a decrease in the hydroxyl band and an increase in the carbonyl band; new signals appeared at 1,389 and 1,140 cm^{-1}, indicating ester bond formation and alterations in hemicellulose. These changes are consistent with the observations of Gomes et al. (2020), who reported similar modifications on the surface of bagasse treated with citric acid.

2.2) Scanning electron microscopy (SEM)

SEM micrographs revealed that the raw bagasse (BC1, Figure 5a) and modified bagasse (BC2, Figure 5b) samples exhibit predominantly fibrous and relatively uniform morphologies (Jaramillo-González, 2025). In BC2, we observed slight cell–wall fractures and partial fiber separation compared with those in BC1. These characteristics suggest that citric acid treatment induces limited structural modifi-cation of the lignocellulosic material, without leading to a clear change in porosity.

Similar morphological changes have been reported in lignocellulosic materials subjected to mild chemical treatments and are associated with changes in surface heterogeneity and the arrangement of functional sites, which can influence interactions with adsorbates (Gomes et al., 2020; Tyagi and Anand, 2024). However, unlike the more aggressive treatments reported in the literature, such as those described by Kerrou et al. (2021), the morphological analysis in the present study did not reveal a significant increase in porosity.

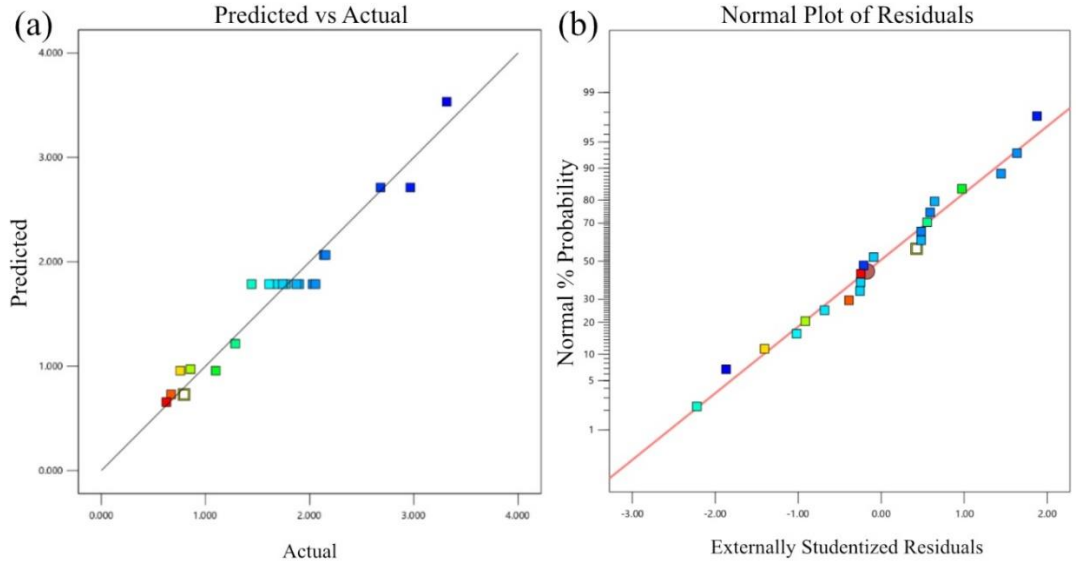


Figure 2 Model validation: a) distribution of predicted versus experimental values for 1/(I1730/I 3400); b) normal probability plot of residuals.

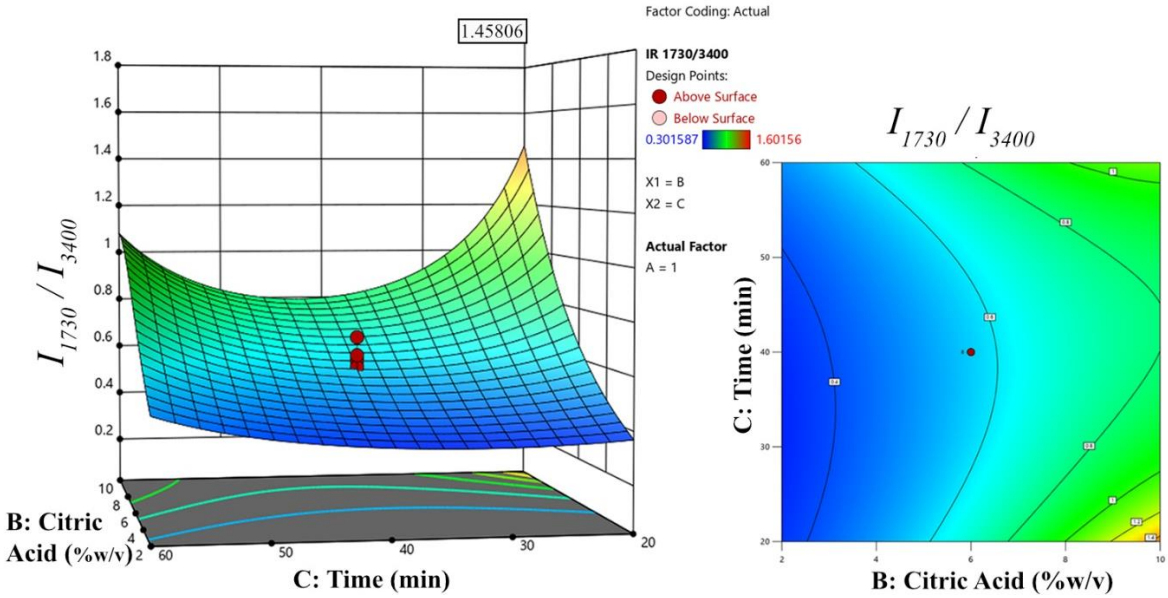


Figure 3 Response surface for the intensity ratio as a function of citric acid concentration and reaction time (Jaramillo-González, 2025).

These observations indicate that under optimized conditions, the contact medium can induce mild surface rearrangements without causing pronounced structural changes detectable by SEM. As noted by Chumpiboon et al. (2022), SEM alone may not detect subtle textural modifications, underscoring the need to complement it with techniques that characterize surface area and porosity for a more detailed evaluation.

2.3) Point of zero charge (pHpzc).

The pHpzc values for BC1 and BC2 are shown in Figure 6. The differences in the pHpzc of BC1 from those in other reports can be explained by variations in adsorbent preparation, adsorbent material origin, and experimental conditions (de Aquino Lima et al., 2024; Kerrou et al., 2021; Mpatani et al., 2020). Citric acid modification shifted the pH to more acidic values; Mpatani et al. (2020) reported a similar trend.

At pH > 3.46, the surface becomes anionic, favoring electrostatic interactions with cationic species and BC1. Conversely, at a pH < 3.46, the surface is positively charged, which favors interactions with anions. The same reasoning applies to BC2. This information is important for establishing working pH values in adsorption experiments.

2.4) Surface acid and basic groups

Table 2 shows the Boehm titration results for BC1 and BC2. Lignocellulosic materials differ in surface acidity because each biomass has distinct proportions of cellulose, hemicellulose, and lignin, and these fractions generate different types and amounts of oxygen-containing groups during natural formation or pretreatment. The total acidity and basicity values for BC1 agree with the presence of carboxylic, lactone, and phenolic–OH groups, which are characteristic of untreated lignocellulosic biomass. Citric acid modification markedly increased the total number of acidic groups and modestly reduced basicity. This observation is consistent with the transformation of basic sites, such as hydroxyl or amine groups, into carboxylic acid functionalities through esterification. These changes, obtained under moderate esterification conditions, align with expected outcomes for lignocellulosic materials subjected to similar functionalization protocols and confirm the successful introduction of additional acidic moieties (Akindolie and Choi, 2023; Nguyen et al., 2019).

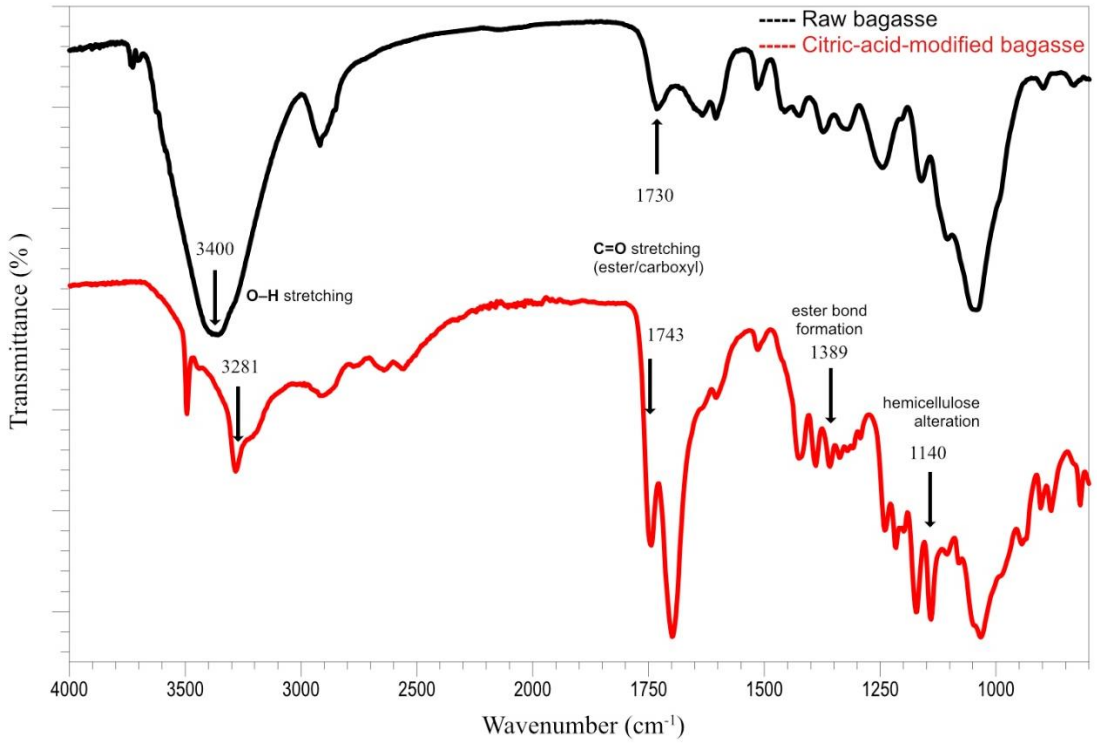


Figure 4 Comparative FTIR spectra of raw bagasse (BC1, black line) and modified bagasse (BC2, red line).

Table 2 Boehm titration for raw (BC1) and modified (BC2) bagasse

Functional group	Raw bagasse	Modified bagasse
Total acidity (NaOH mmol g^{-1})	1.98 ± 0.05	5.19 ± 0.03
Basicity (HCl mmol g^{-1})	0.39 ± 0.03	0.31 ± 0.05

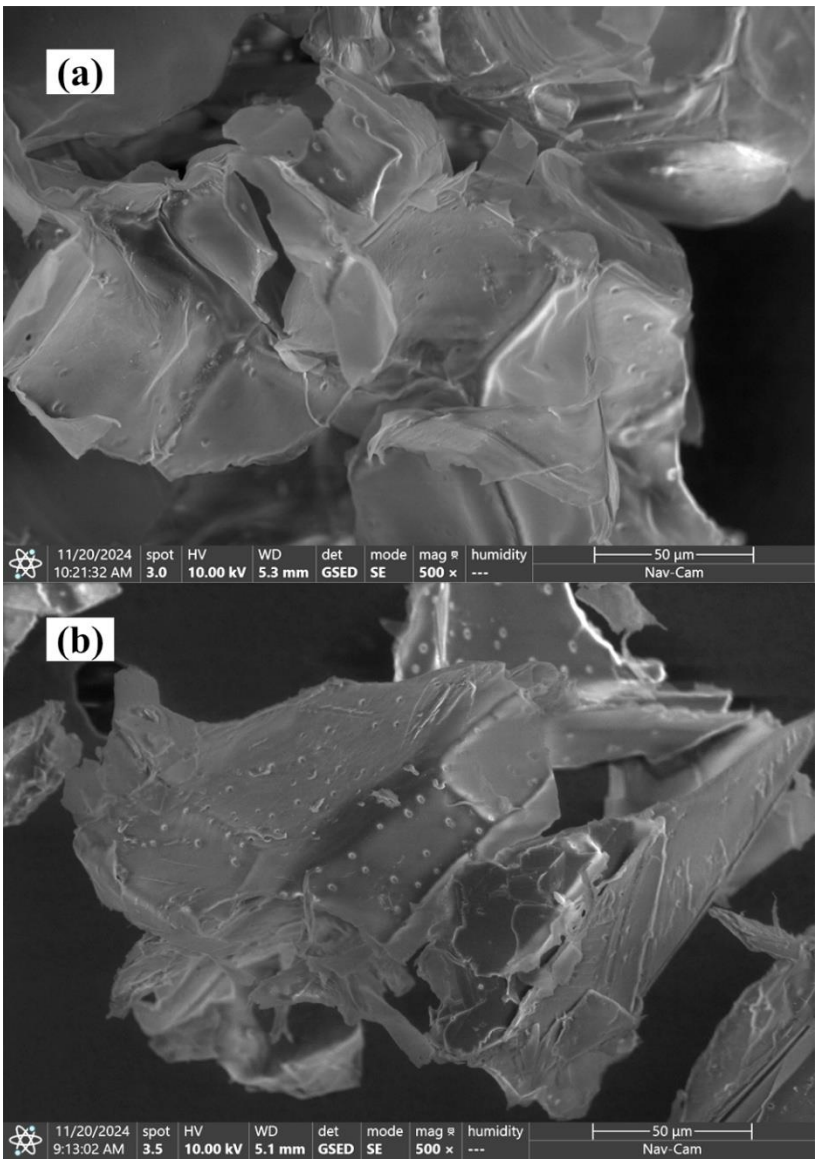


Figure 5 SEM micrographs (500×) of sugarcane bagasse before and after chemical modification: (a) raw bagasse (BC1); (b) bagasse modified with citric acid (BC2).

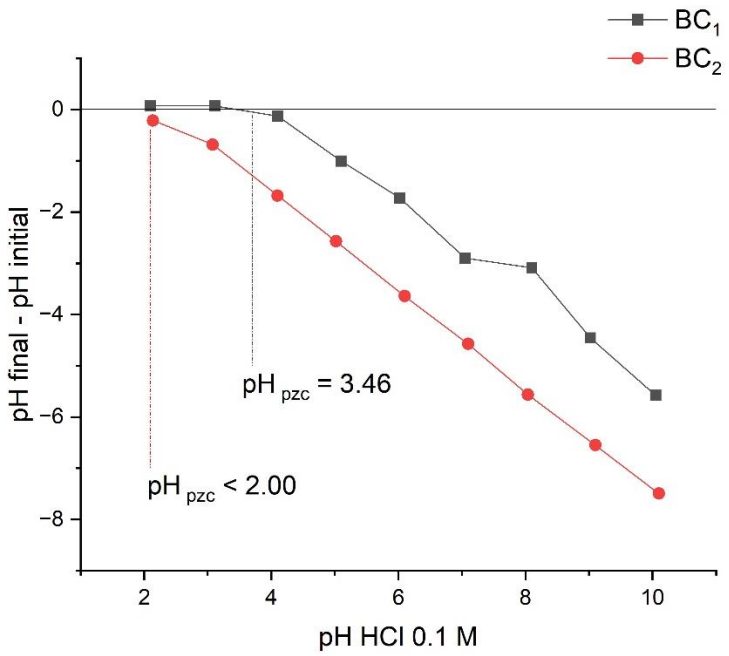


Figure 6 Points of zero charge for BC1 and BC2.

3) Vinasse characterization

The Panamanian technical regulation DGNTI-COPANIT 35-2019 establishes discharge limits on continental and maritime water bodies for the main physicochemical water quality parameters (MICI, 2019). Table 3 shows some of these parameters for the vinasse sample and the corresponding discharge limit. As shown, all the parameters exceed the permissible limits: pH alters the physicochemical properties of water bodies, which, in turn, negatively affects aquatic life. Vinasse's low pH is due mainly to organic acids. High COD values indicate high organic loads. This characteristic makes the effluent recalcitrant and reduces available oxygen, which negatively affects aquatic life. The high phenol content of vinasse is due mainly to tannins and condensed tannins, which are part of the organic load. Colored effluents block light transmission and negatively affect aquatic ecosystems. Melanoidins, phenols, caramels, and furan derivatives are responsible for the color of vinasse (Caballero et al., 2021; 2024; de Aquino Lima et al., 2024).

Additionally, the vinasse parameters exceed the limits set by the technical regulation governing the direct discharge of effluents into wastewater collection systems, DGNTI-COPANIT 39-2000 (MICI, 2008).

4) Biosorption assays

4.1) Contact time

The kinetic behavior of tannin removal efficiency was evaluated from experimental profiles as a function of contact time and from the statistical analysis of mean removal values (Figure 7). For both adsorbents, a rapid initial phase was observed during the first 30 minutes, which can be associated with the availability of active sites on the material surface (Kerrou et al., 2021).

Table 3 Physicochemical characterization of vinasse

Parameter	Unit	Result	DL[a]
pH	-	4.70	5.5 – 9.0
COD	mg L^{-1}	85507	≤ 100
Turbidity	NTU	> 800	≤ 40
Total solids	mg L^{-1}	79000	≤ 500
Conductivity	µS cm^{-1}	22120	≤ 2000
Color	mg L^{-1}	> 500	No visible color
Total tannin	mg L^{-1}	389.05	≤ 0.5

Remark: [a] Wastewater discharge limits (DGNTI-COPANIT 35-2019)

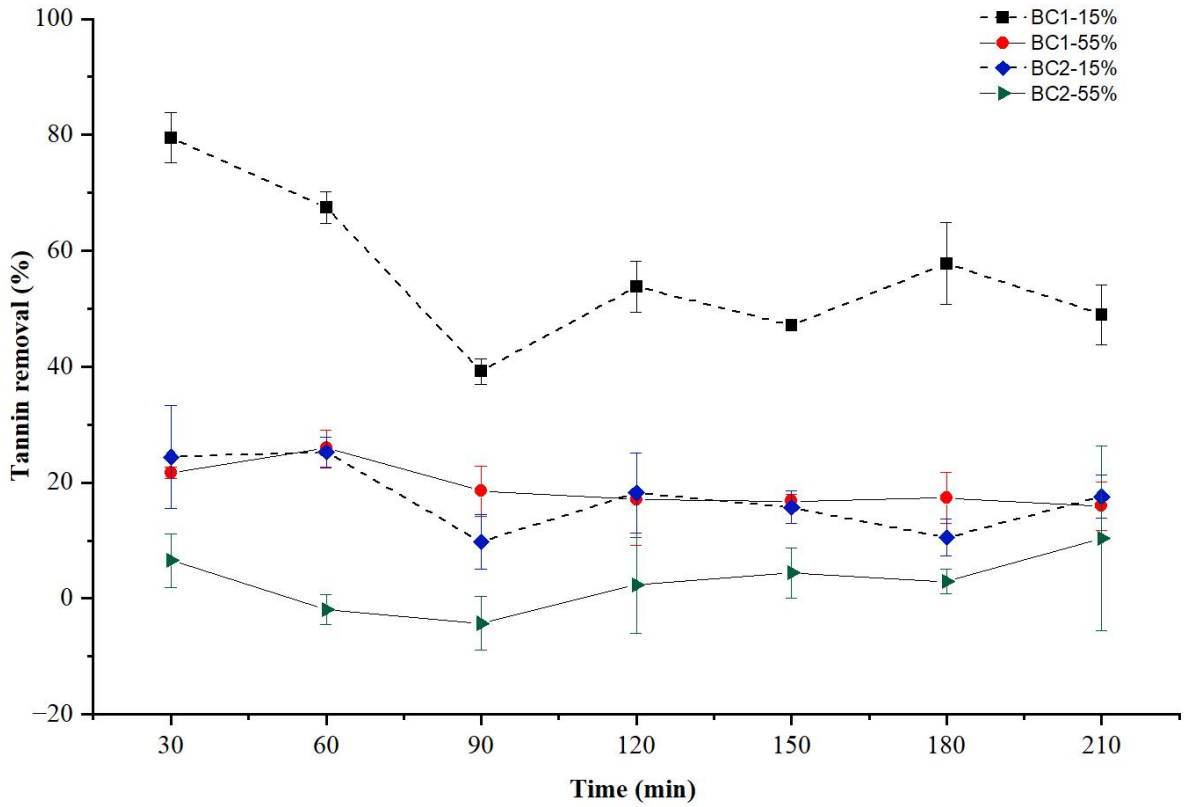


Figure 7 Kinetics of total tannin removal efficiency in vinasse using raw bagasse (BC1) and modified bagasse (BC2) at two concentrations (15% and 55% v/v). The values represent the mean ± standard deviation (n = 3) (Adapted from Jaramillo-González (2025)).

Analysis of variance (ANOVA) and Tukey's HSD test revealed that for BC1 and BC2 in 15% vinasse, some contact times differed significantly ($p < 0.05$). However, from 120 minutes onward, we observed no statistically significant differences in mean removal values, indicating a dynamic equilibrium. For 55% vinasse, we observed no statistically significant differences in mean removal values across the evaluated contact times for either BC1 or BC2.

In this study, we assessed the effect of the effluent concentration by comparing 15% and 55% vinasse under identical operating conditions. Statistical analysis revealed lower removal efficiencies at higher effluent concentrations for both adsorbents, indicating that higher adsorbate concentrations negatively affect the adsorption performance. Chingono et al. (2018) reported a similar trend for phenol-rich sugarcane vinasse systems, where removal efficiency decreased with increasing effluent concentration. Miguel-Gallo et al. (2017) emphasized that the adsorption kinetics of sugarcane-derived materials are strongly influenced by operational parameters, including contact time, pH, and initial concentration. On the basis of these results, we selected a contact time of 120 minutes for subsequent biosorption optimization experiments (Jaramillo-González, 2025).

4.2) Optimization of biosorption conditions

4.2.1) Raw bagasse (BC1)

Equation 6 represents the reduced quadratic model in coded units, with a power transformation, for tannin biosorption in vinasse using raw bagasse (BC1). The analysis of variance (ANOVA) results revealed that the model is highly significant ($F = 132.32$, $p < 0.0001$), indicating a strong relationship among the variables. The lack-of-fit F value of 1.40 indicates that the lack of fit is not statistically significant compared with the pure error ($p = 0.4250$). Overall, the model showed a good fit ($R^2 = 0.9893$; adjusted $R^2 = 0.9818$; predicted $R^2 = 0.9479$) and an adequate precision of 35.67, suggesting reliable predictive capability.

The model demonstrates a good overall fit across the entire range of the variable, without any pronounced systematic bias (Figure 8 a). Additional analyses (graphs not shown) confirm that the outlier exhibits moderate deviation and does not substantially compromise normality.

The most influential factor was vinasse dilution ($p < 0.0001$), with a negative effect: a higher vinasse concentration was associated with lower removal efficiency (Jaramillo-González, 2025). Reducing the vinasse concentration decreases the amount of interfering substances that compete with phenols for adsorption sites. Conversely, higher vinasse concentrations intensify this competition, thereby reducing the selective removal efficiency of phenols (Christofoletti et al., 2013). pH (factor A) was not significant in its linear term ($p = 0.7703$) but was significant in its quadratic term ($p < 0.0001$), indicating a nonlinear relationship with removal. Bagasse (factor B) did not have a significant effect ($p > 0.05$).

$$(\text{Tannin removal }\%)^{1.91} = 2521.54 + 12.72A + 0.0541B - 1255.58C - 84.31AC - 86.39BC + 492.90A^2 - 234.08C^2 \quad \text{(Eq.6)}$$

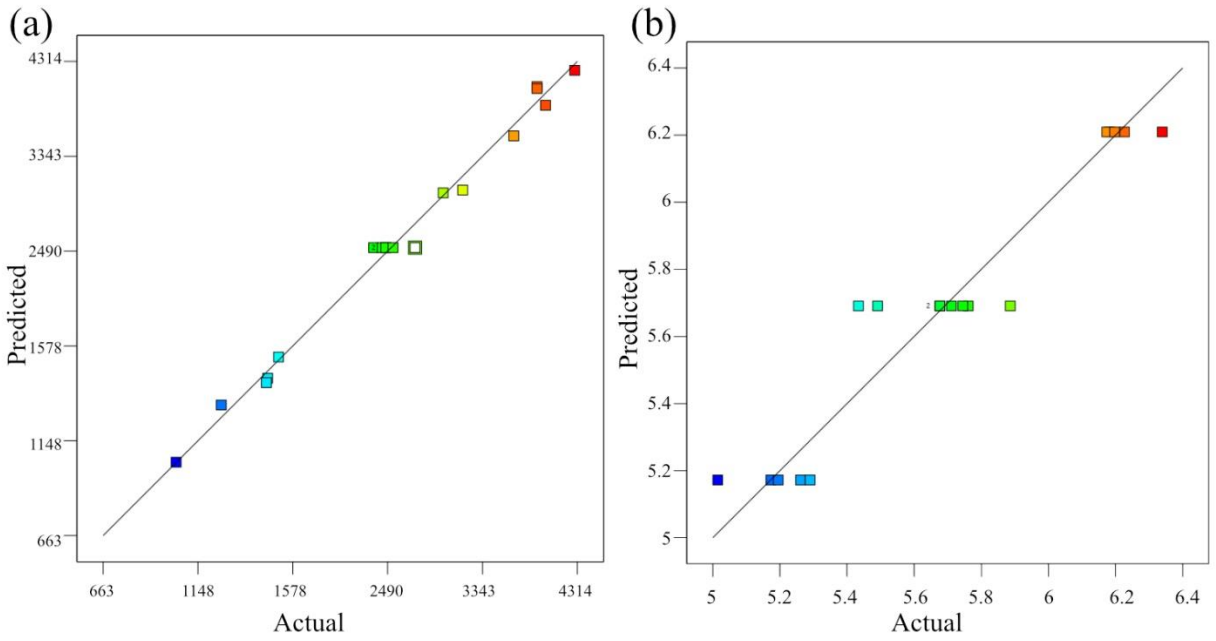


Figure 8 Model diagnostics: distribution of predicted versus actual values for vinasse biosorption on a) raw sugarcane bagasse and b) modified sugarcane bagasse.

The optimal conditions for BC1 were a pH of 7.0, 0.4 g of bagasse, and 50% vinasse, yielding a removal efficiency of 79.07% at a desirability of 0.979. These results were experimentally confirmed, with an observed removal of 79.73%. The response surface (Figure 9) shows the interaction between the pH (A) and vinasse concentration (C); as the vinasse concentration decreased, the removal efficiency increased, whereas the effect of the pH followed a quadratic trend.

This behavior can be attributed to the influence of pH on the surface charge of raw bagasse and the protonation state of phenolic hydroxyl groups in tannins and related phenolic compounds in vinasse. For BC1, the optimal pH for removal was 7.0, which is above its point of zero charge (pHpzc) of 3.46. Under these conditions, the raw bagasse surface is expected to carry a net negative charge. However, since most phenolic hydroxyl groups remain largely nondissociated at this pH, electrostatic attraction between bagasse and tannins is unlikely to be the primary removal mechanism. Instead, nonelectrostatic interactions—such as hydrogen bonding, hydrophobic interactions, π–π interactions with lignin aromatic domains, and nonspecific physical adsorption on heterogeneous lignocellulosic surfaces—are likely to play a more significant role (Koopmann et al., 2020; Soto et al., 2011).

Several studies on phenolic compound adsorption have shown that pH affects removal efficiency by altering the adsorbent surface charge, the acid–base behavior of phenolic groups, and competition in the liquid phase (Gholizadeh et al., 2013; Kerrou et al., 2021). Accordingly, the adsorption behavior observed in the present study likely reflects the combined effects of raw bagasse surface charge, the expected protonation state of tannin phenolic groups, and the competitive nature of the vinasse matrix.

4.2.2) Modified bagasse (BC2)

For BC2, the reduced linear model was highly significant ($F = 196.26$, $p < 0.0001$), suggesting a strong relationship between the variables. The lack-of-fit F value of 0.4658 indicates that the lack of fit is not statistically significant compared with the pure error ($p = 0.8565$). The model showed a good fit ($R^2 = 0.9246$; adjusted $R^2 = 0.9199$; predicted $R^2 = 0.9091$) and an adequate precision of 26.58, suggesting that the model has a reliable predictive ability. Equation 7 shows the reduced model in coded units.

The Predicted vs. Actual plot (Figure 8b) confirms that the statistical model for the transformed variable $(\text{tannin removal})^{0.42}$ exhibits a good overall fit. The data points are distributed close to the identity line across the entire experimental range, with small, randomly distributed prediction errors. Homoscedasticity is confirmed (plots not shown); the error variance is approximately constant across the range. The power transformation improved the model fit, and these results validate its application for predicting and optimizing tannin removal within the experimental space studied.

$$(\text{Tannin removal }\%)^{0.42} = 5.69 - 0.5185C \quad \text{(Eq. 7)}$$

Only vinasse dilution was significant ($p < 0.0001$); neither the pH nor the bagasse dosage had a statistically significant influence within the studied range. These results indicate that BC2 tannin removal was governed mainly by the vinasse concentration rather than the solution pH or adsorbent dosage. The removal efficiency decreased linearly as the vinasse concentration increased, as shown in Figure 10, where the negative slope reflects the dominant effect of dilution on the material's adsorptive capacity (Jaramillo-González, 2025). Although the pH was not statistically significant, the numerical optimization resulted in a pH of 3.0, 0.2 g of bagasse, and 50% vinasse, with a predicted removal of 77.35% (desirability = 1.000). Under these conditions, the experimental value was 80.30%, confirming the validity of the model.

In contrast to that in BC1, tannin removal in BC2 depended primarily on the vinasse concentration. This suggests that the retention of BC2 tannins was not primarily controlled by electrostatic interactions within the evaluated pH range. Instead, citric acid modification likely generated a heterogeneous surface containing ester, carboxylic, carbonyl, hydroxyl, and lignin-associated aromatic domains that can interact with tannins and related phenolic constituents through multiple nonelectrostatic mechanisms. These interactions may include hydrogen bonding, hydrophobic interactions, π–π interactions with aromatic structures of lignin, and nonspecific physical adsorption. Therefore, the adsorption process in BC2 can be interpreted as a mixed mechanism dominated by surface interactions and matrix competition rather than by pH-dependent electrostatic attraction. The selection of a pH of 3.0 should be interpreted as an operational setting determined through numerical optimization rather than as evidence that an acidic pH was a statistically significant controlling factor.

Recent reviews have emphasized the importance of developing biomass-derived adsorbents that maintain adsorption efficiency under nonideal conditions, including acidic pH and complex, multicomponent effluents (Tyagi and Anand, 2024). In this context, the experimental results for BC2 indicate that citric acid-modified bagasse demonstrates functional versatility for treating sugarcane vinasse.

We compared the means between the two groups (BC1 and BC2) using a two-tailed paired Student's t test ($\alpha = 0.05$) after confirming homogeneity of variance. The mean difference was −2.262 units (BC1− BC2),

with t = −2.172 (df = 17) and p = 0.044. Because the observed |t| (2.172) exceeded the two-tailed critical value (2.110) and the 95% confidence interval for the difference (−4.460, −0.065) excluded zero, we rejected the null hypothesis of equal means. The modified bagasse had a significantly greater mean (63.327 vs. 61.065), representing an approximate 3.7% increase, with a type I error risk less than 4.

On the basis of its pH tolerance within the studied range and the higher removal efficiency observed in the statistical analysis, modified bagasse emerges as a better alternative than unmodified bagasse.

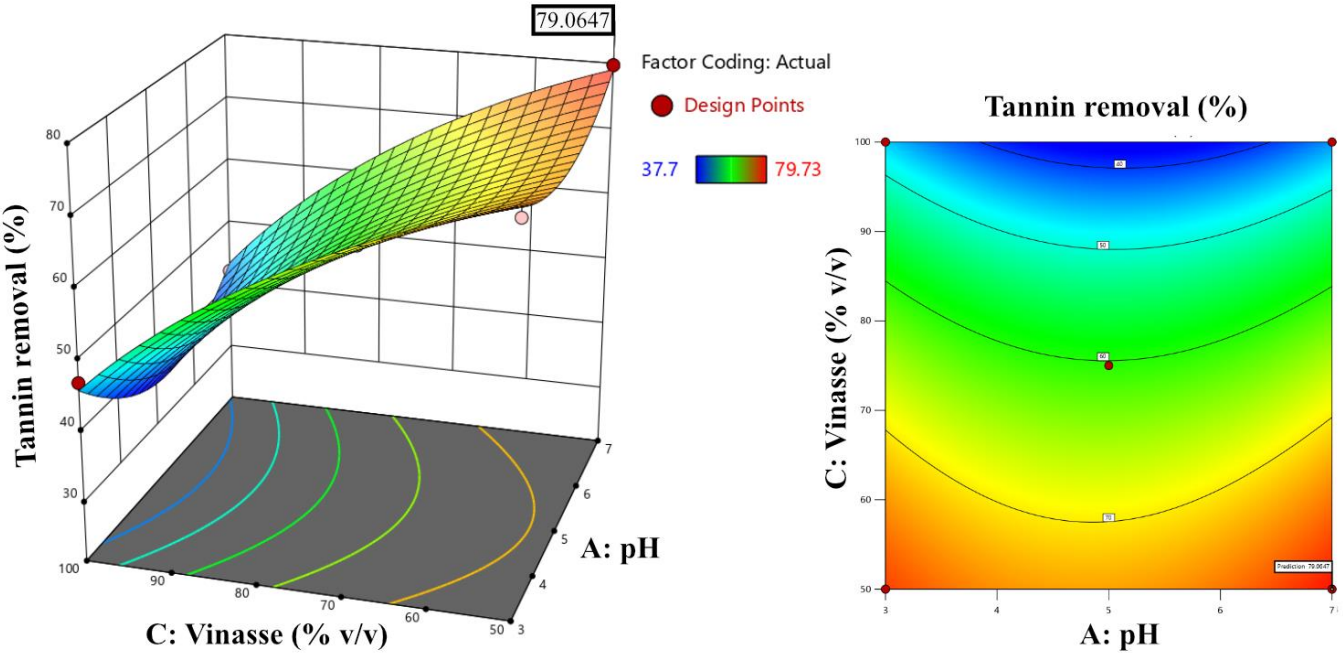


Figure 9 Response surface for tannin removal: interaction between pH (A) and vinasse concentration (C).

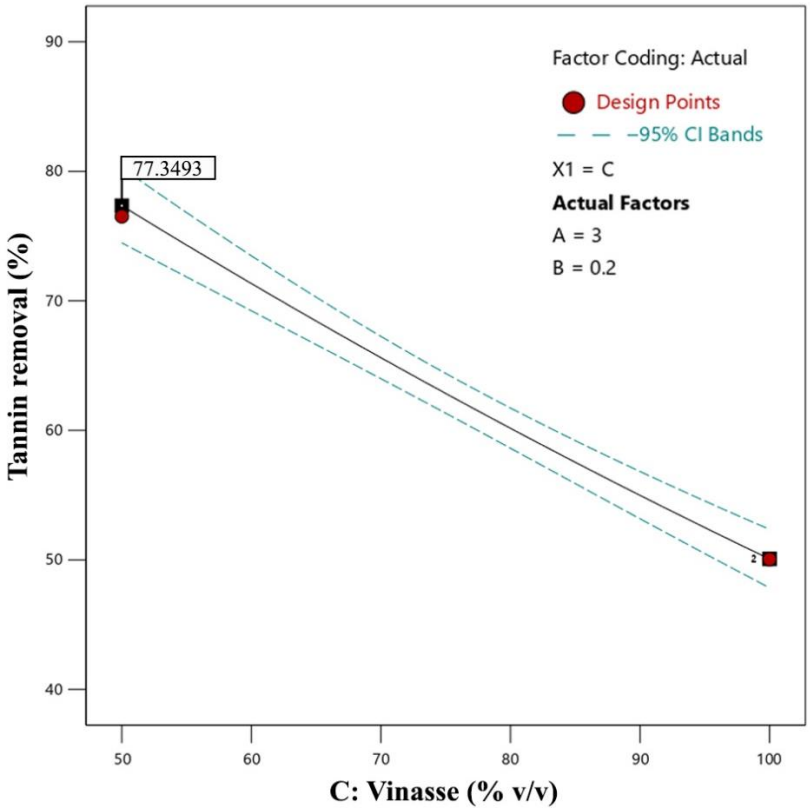


Figure 10 Effect of vinasse dilution on tannin removal efficiency using modified bagasse (Jaramillo-González, 2025).

The spent adsorbents were also characterized. Following biosorption, changes were observed in the characteristic FTIR bands of both (Figure 11). In spent BC1, the O–H stretching band shifted from 3,400 to 3,350 cm^{-1}, indicating stronger hydrogen bonding; this suggests that the O–H bond weakens as it donates more electron density to the hydrogen bond. In other words, the O–H groups of the adsorbent form stronger hydrogen bonds with the adsorbate. The carbonyl band shifted slightly from 1,721 to 1,726 cm^{-1}; this minor change suggests a weak interaction with the carbonyl group, possibly through low-intensity C=O···H hydrogen bonds. These spectral regions are typically associated with hydroxyl groups in lignocellulosic macromolecules (cellulose, hemicellulose, and lignin), as well as with the stretching vibrations of carboxyl and lignin ester groups.

Additional changes were detected in the C–O/C–O–C region, particularly between 1,034 and 1,050 cm^{-1}, corresponding to glycosidic deformations and vibrations of cellulosic components. This suggests interactions with cell wall polysaccharides, possibly via hydrogen bonding with the cellulose ring oxygens or hydrophobic interactions with the polysaccharide backbone (de Aquino Lima et al., 2024; Mpatani et al., 2020).

For spent BC2, more pronounced changes were observed: the O–H band shifted from 3,281 to 3,382 cm^{-1}. This is consistent with the hydrogen-bonding interactions between the adsorbent and adsorbate, in which the –OH groups of the adsorbent act as donors or acceptors. In the carbonyl region, the dual bands at 1,743 and 1,699 cm^{-1} merged into a single band centered near 1,716 cm^{-1}, suggesting that both carbonyl environments are affected—possibly because of interactions between carboxylic groups and phenolic groups via C=O···H–O hydrogen bonds or because of slight electronic reorganization of the ester environment from the incorporated citric acid.

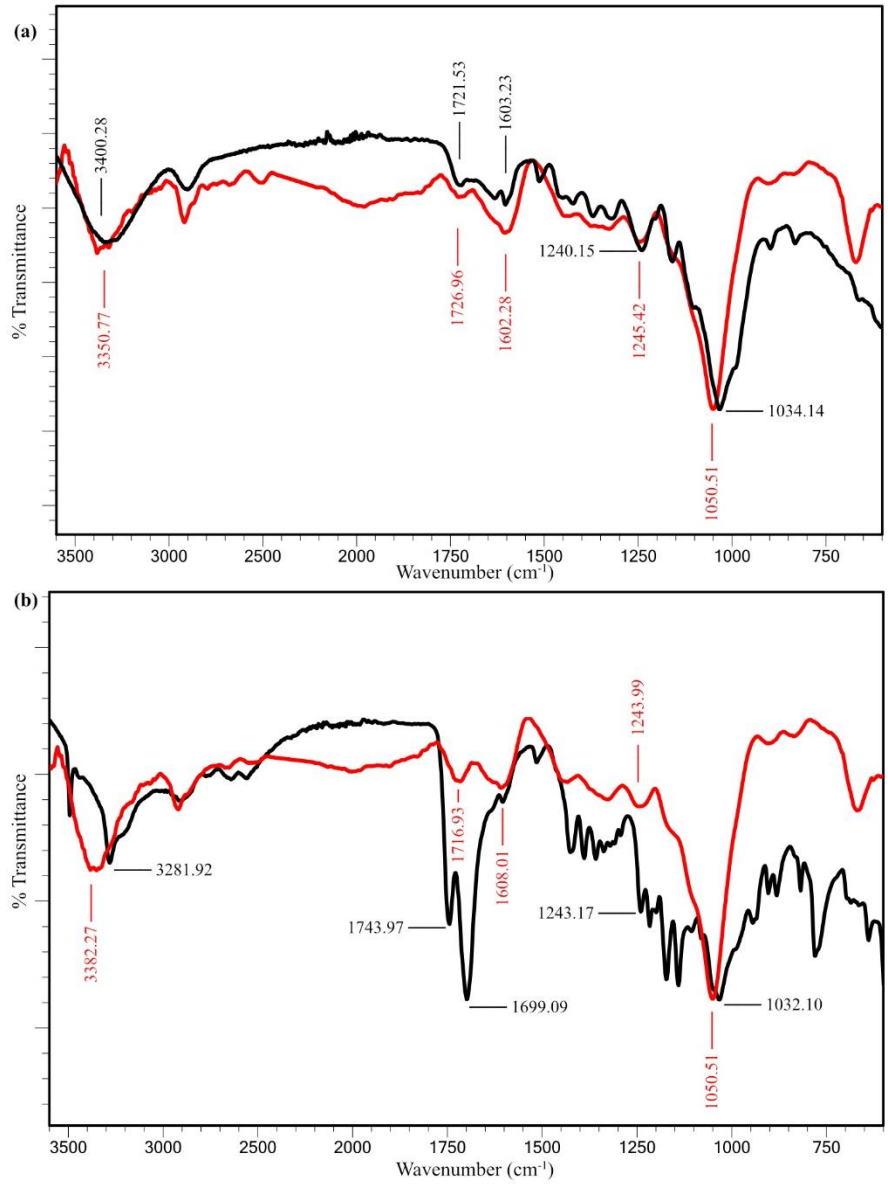


Figure 11 Comparative FTIR spectra of raw and modified bagasse after the biosorption process. (a) BC1: black, raw bagasse; red, spent BC1; (b) BC2: black, citric acid-modified bagasse; red, spent BC2.

These spectral shifts indicate modifications in the chemical environment of hydroxyl, carbonyl, and other oxygenated groups, supporting their potential involvement in specific interactions between the bagasse surface and vinasse components during biosorption rather than the definitive formation of new covalent bonds (de Aquino Lima et al., 2024; Mpatani et al., 2020).

Confocal microscopy revealed autofluorescence in the spent bagasse samples (Figure 12). In BC1 and BC2 treated only with water, a basal level of fluorescence was recorded, whereas samples exposed to vinasse showed higher emission intensities in the 430–470 nm (blue) and 500–600 nm (green) ranges, attributed to phenolic compounds such as tannins. This increased signal in the spent bagasse provides complementary evidence of phenolic molecules retained on the material surface.

Donaldson (2020) highlights that the autofluorescence of natural aromatic compounds (such as lignin, flavonoids, and tannins) enables the visualization of their distribution in lignocellulosic matrices without the need for external markers. In this study, the response observed in the modified bagasse suggests that esterification not only increases surface accessibility (SEM) but also enhances interactions with phenols, as detected through spectral techniques. The differences observed between the control samples (water) and those treated with vinasse may therefore be associated with the surface retention of phenolic compounds, suggesting the potential use of autofluorescence as a qualitative indicator of adsorption processes (Jaramillo-González, 2025).

5) Equilibrium and kinetic studies

Modified bagasse was selected as the primary material for the adsorption and kinetic studies. On the basis of the optimized conditions for determining the amount of adsorbate and the pH, the experimental design detailed in the materials and methods section (biosorption assays: evaluation of contact time) was repeated using 50% v/v (194.5 mg L^{-1}) vinasse at pH 3 and 30 °C. The kinetic profile is shown in Figure 13. The removal efficiency graph indicates rapid adsorption within the first 30 minutes, followed by a plateau at approximately t = 120 minutes, suggesting that equilibrium was reached. The adsorption capacity (qt) exhibited the same trend, confirming that the process stabilized.

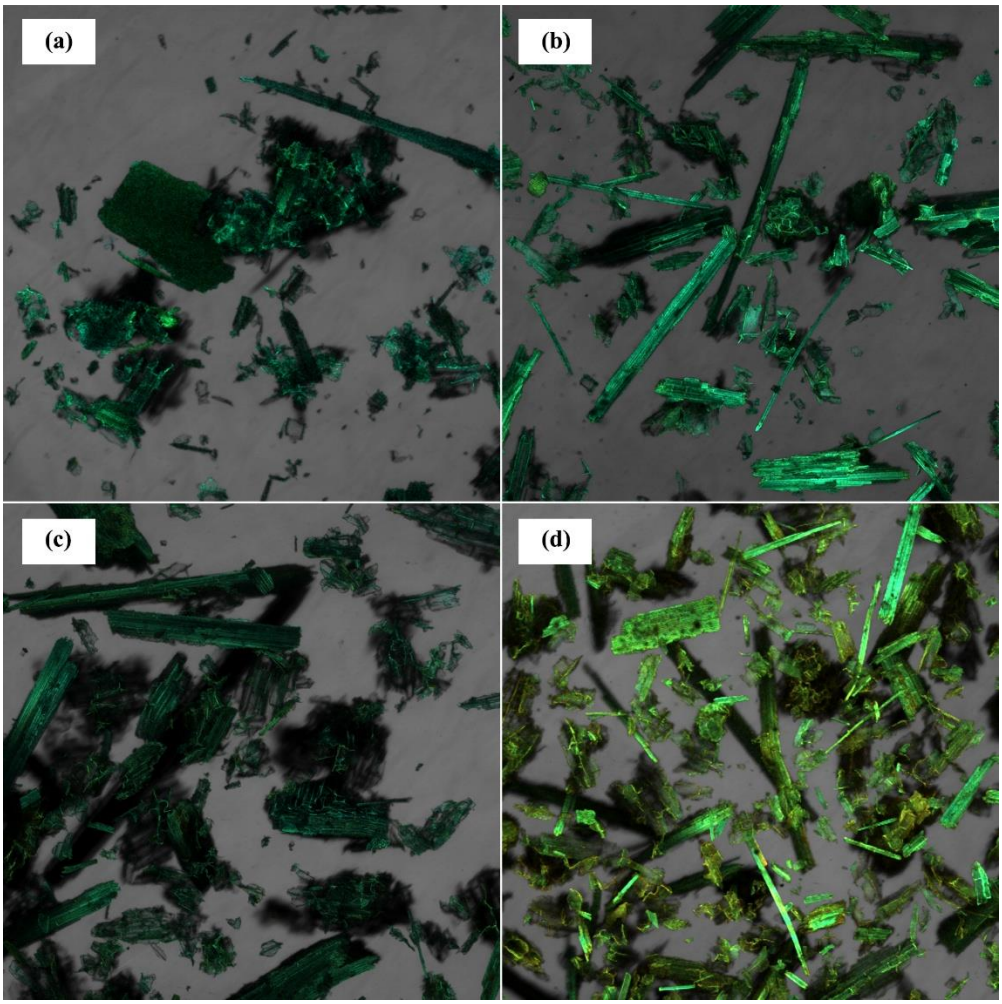


Figure 12 Confocal microscopy of spent adsorbents: a) BC1 with water, b) spent BC1 with 50% vinasse, c) BC2 with water, and d) spent BC2 with 50% vinasse (Jaramillo-González, 2025).

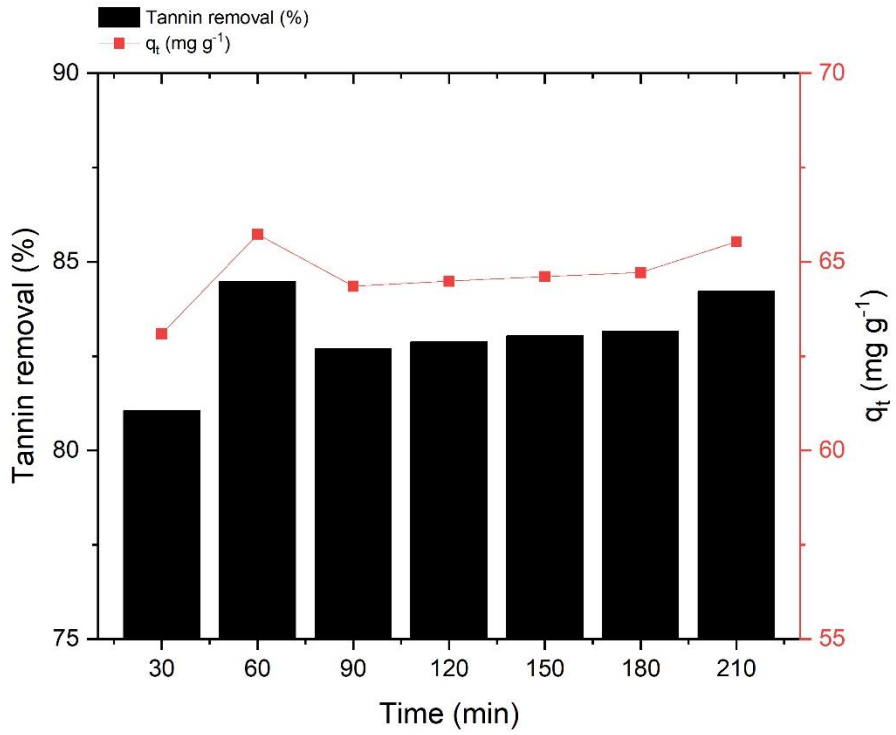


Figure 13 Kinetic profile of tannin removal efficiency and adsorption capacity.

The experimental equilibrium adsorption capacity (q_e,exp) was determined by averaging the qt values at the equilibrium plateau (t ≥ 120 minutes), where the system showed no significant variation. The q_e,exp was 64.836 mg g^{-1}, the average equilibrium concentration (Ce) was 64.87 mg L^{-1}, and the average tannin removal efficiency was 83.33%. Table 4 compares the theoretical q_e values obtained from each model with the experimental values, along with the corresponding fitting parameters. The pseudo-second-order (PSO) model provided an excellent description of the kinetics, with R^2 = 0.9998 and a relative error of only 1.02% between q_e (65.5 mg g^{-1}) and q_e, exp (64.836 mg g^{-1}). This result should be interpreted as evidence that the adsorption rate depends strongly on the availability of active surface sites rather than as definitive evidence of covalent chemisorption (Hubbe et al., 2019; Vareda, 2023). The rate constant, $k_2 = 1.664\times10^{-2}$ g mg^{-1} min^{-1}, reflects the adsorption rate and allows for the estimation of the initial adsorption rate: $h_0 = k_2 \cdot q_e^2 = 1.664\times10^{-2}$ $(65.5)^2 \approx 71.4$ mg g^{-1} min^{-1}.

Intraparticle diffusion is not the sole rate-limiting mechanism, and external surface adsorption or boundary-layer effects contributed significantly to the initial uptake, as indicated by the Weber–Morris model (R^2 = 0.32, C = 61.61 mg $g^{-1} \neq 0$). The high value of the constant C suggests that most of the adsorption occurs rapidly during the initial stage before intraparticle diffusion becomes the limiting step (Chakraborty et al., 2023; Papirio et al., 2017). This finding is consistent with the observation of rapid removal during the first 30 minutes, followed by a plateau at approximately 120 minutes.

For the adsorption equilibrium studies, we used the Langmuir (Eq. 8), Freundlich (Eq. 9), and Temkin (Eq. 10) isotherm models:

$$q_e = q_m K_L C_e/(1 + K_L C_e) \quad \text{(Eq. 8)}$$

$$q_e = K_F C_e^{1/n} \quad \text{(Eq. 9)}$$

$$q_e = (RT/b_T)\ln(A_r C_e) \quad \text{(Eq. 10)}$$

where q_m is the maximum monolayer adsorption capacity (mg g^{-1}); K_L is the Langmuir affinity constant (L mg^{-1}); K_F and *n* are the Freundlich constants related to the adsorption capacity and intensity, respectively; R is the universal gas constant (8.314 J mol^{-1} K^{-1}); K is the absolute temperature; and b_T and A_T are the Temkin constants associated with the heat of adsorption (J mol^{-1}) and equilibrium binding (L mg^{-1}), respectively.

The adsorption isotherms of vinasse on citric acid-modified bagasse at the following experimental conditions are shown in Figure 14: temperature, 35 °C; pH, 3; bagasse dose, 0.1 g; volume, 20 mL; particle size, 500 µm; and contact time, 150 rpm (120 minutes). Model isotherm parameters are shown in Table 5.

Table 4 Kinetic parameters obtained from the adsorption model fitting

Kinetic model	$q_{e,teo}$ (mg g^{-1})	$q_{e,exp}$ (mg g^{-1})	R^2	Kinetic parameters
Pseudo first-order	6.00	64.836	0.0800	k_1 = 0.0080 min^{-1}
Pseudo second-order	65.50	64.836	0.9998	k_2 = 1.664x10^{-2} g mg^{-1} min^{-1}
Weber-Morris intraparticle diffusion	---	64.836	0.3200	k_{id} = 0.271 mg g^{-1} $min^{-1/2}$ C = 61.61 mg g^{-1}

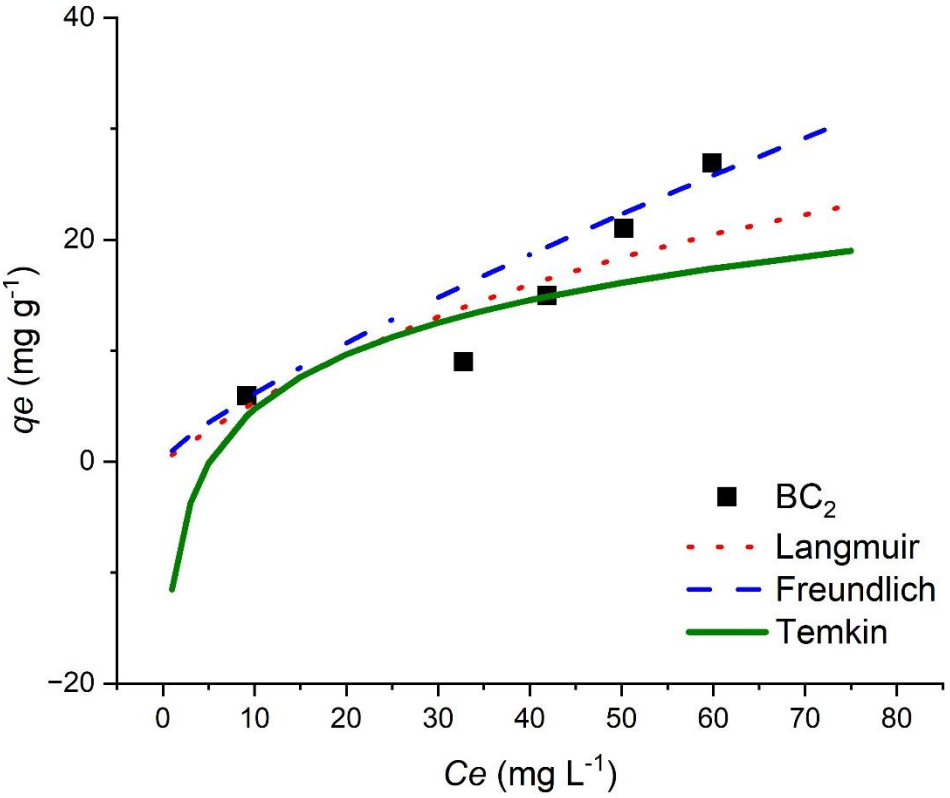


Figure 14 Isothermal adsorption of vinasse on citric acid-modified bagasse.

Table 5 Equilibrium isotherm parameters at different temperatures

Isotherm model	Temperature (°C)	R^2	Key parameters
Langmuir	30	0.891	q_{max} = 52.63 mg g^{-1}; K_L = 0.0089 L mg^{-1}
	35	0.952	q_{max} = 47.62 mg g^{-1}; K_L = 0.0126 L mg^{-1}
	40	0.621	q_{max} = 38.46 mg g^{-1}; K_L = 0.0198 L mg^{-1}
Freundlich	30	0.972	K_F = 0.586; *1/n* = 0.897
	35	0.993	K_F = 0.968; *1/n* 0.820
	40	0.712	K_F = 2.406; *1/n* 0.432
Temkin	30	0.958	b_T = 411.5 J mol^{-1}; A_T = 0.148 L mg^{-1}
	35	0.981	b_T = 362.3 J mol^{-1}; A_T = 0.196 L mg^{-1}
	40	0.726	b_T = 379.1 J mol^{-1}; A_T = 0.387 L mg^{-1}

The Freundlich model exhibited the highest overall R^2 values (0.972 at 30 °C and 0.993 at 35 °C), outperforming both the Langmuir and Temkin models at the temperatures with the greatest experimental reliability. The 1/n values below 1 at all temperatures confirm favorable adsorption on a heterogeneous surface (Papirio et al., 2017), which is consistent with the physical behavior of natural or activated carbon-based adsorbents and potentially multilayer adsorption. The progressive increase in K_F with increasing temperature (0.586 → 0.968 → 2.406) is consistent with an endothermic process (Hu et al., 2023; Wang and Guo,

2020). The Langmuir model, which assumes a homogeneous monolayer, is less realistic for this system and yields the lowest R^2 values. The Temkin model fit well at 30 °C and 35 °C but decreased markedly at 40 °C.

The combined kinetic, equilibrium, and FTIR results suggest that tannin biosorption occurs through a mixed adsorption mechanism. Pseudo-second-order kinetics and Weber–Morris analysis indicate that intraparticle diffusion plays a role but is not the only rate-limiting step. The data fits the Freundlich isotherm better, supporting adsorption on a heterogeneous surface with varying site affinities. Additionally, the shifts in the O–H, C=O, and C–O/C–O–C bands in the FTIR spectra indicate the involvement of surface functional groups.

To further support this discussion, $\Delta H°$ was calculated (Chakraborty et al., 2023). The value of $\Delta H° = +38.5$ kJ mol^{-1} lies within the typical range for hydrogen bonding interactions (10–40 kJ mol^{-1}), which is consistent with the changes observed in the FTIR spectra and falls within the interval conventionally associated with intermediate-energy adsorption (Inglezakis and Zorpas, 2012). This value, together with the spectroscopic evidence, rules out both weak physisorption (pure van der Waals forces) and strong chemisorption (covalent bond formation).

Conclusions

We used a statistical optimization methodology to synthesize citric acid-modified sugarcane bagasse and determine the optimal adsorption parameters for removing tannins from vinasse. FTIR spectroscopy confirmed structural modifications in the bagasse attributed to citric acid esterification. Compared with the raw material, the modified bagasse showed markedly improved adsorption performance, as shown by enhanced pH tolerance and higher removal efficiency, demonstrating its suitability for treating complex, tannin-rich effluents.

Kinetic, equilibrium, and FTIR analyses collectively suggest that adsorption in modified bagasse is governed by a combination of physical interactions, including hydrogen bonding, and relatively weak, specific surface interactions, rather than a single dominant pathway.

This study advances the knowledge base needed to develop sustainable valorization and treatment strategies for sugarcane industry residues.

Further research should focus on comprehensive surface area and porosity characterization, as well as on evaluating the regeneration and long-term stability of modified materials. Additionally, a systematic investigation of the effects of varying citric acid concentrations during the modification process is recommended to establish a robust experimental foundation for future assessments of technical, economic, and environmental feasibility.

Acknowledgements

This study was funded by the National Secretariat of Science, Technology and Innovation (SENACYT), Panama, project APY-NI-2024A-14. Authors express special thanks to Ingenieria Prego S.A. for their assistance in acquiring and analyzing the FTIR spectra, as well as to the Institute for Scientific Research and High Technology Services (INDICASAT AIP) for providing support with the scanning electron microscopy (SEM) and confocal microscopy analyses. Finally, the authors thank Professor Víctor Jiménez for his valuable advice in statistical analyses, Mr. Jesus Pitty and his farm collaborators for supplying the sugarcane bagasse, and the Central Industrial Chiricana (CICHISA) for providing the vinasse samples.

Data availability statement

Information and data used in the study will be disclosed upon request.

Author ORCID

Nicomedes Ariel Jaramillo-González: 0000-0002-1342-0624
Mónica Miranda: 0000-0003-0576-6972
Jorge Ceballos: 0000-0003-0556-9493
Rosa Elena Caballero: 0000-0002-8888-524X

Author contributions

Nicomedes Ariel Jaramillo-González: Methodology, Validation, Formal analysis, Investigation, Writing – Original draft, Writing – Review & editing, Visualization, Funding acquisition
Mónica Miranda: Investigation, Writing – Review & editing
Jorge Ceballos: Formal analysis, Writing – Review & editing
Rosa Elena Caballero: Conceptualization, Methodology, Formal analysis, Writing – Review & editing, Supervision

Conflicts of interest

The authors declare that there are no conflicts of interest in competing financial or personal relationships that could have appeared to influence the work reported in this work.

References

Ajala, E. O., Ighalo, J. O., Ajala, M. A., Adeniyi, A. G., & Ayanshola, A. M. (2021). Sugarcane bagasse: A biomass sufficiently applied for improving global energy, environment and economic sustainability. *Bioresources and Bioprocessing*, *8*, 87.

Akindolie, M. S., & Choi, H. J. (2023). Acid modification of lignocellulosic derived material for dye and heavy metals removal: A review. *Environmental Engineering Research*, *28*(2), 210574.

APHA/AWWA/WEF. (2017). *Standard methods for the examination of water and wastewater* (23rd ed.).

Washington, D.C.: American Public Health Association (APHA), American Water Works Association (AWWA), and Water Environment Federation (WEF).

Anku, W. W., Mamo, M. A., & Govender, P. P. (2017). Phenolic compounds in water: Sources, reactivity, toxicity and treatment methods. In Soto-Hernandez, M., Palma-Tenango, M., & Garcia-Mateos, R. (Eds.), *Phenolic compounds - Natural sources, importance and applications* (pp. 419–443). IntechOpen.

AOAC. (2005). *Official methods of analysis* (18th ed.). Association of Official Analytical Chemists.

Aruna, Bagotia, N., Sharma, A. K., & Kumar, S. (2021). A review on modified sugarcane bagasse biosorbent for removal of dyes. *Chemosphere*, *268*, 129309.

Atencio, V. R., Goebel, F. R., Salazar, J. D., & Guerra, A. (2020). Biotecnologia aplicada a la produccion de cana de azucar en Panama: Una vision general. *Revista Cientifica Universitaria CENTROS*, *9*(2), 128–143.

Bakatula, E. N., Richard, D., Neculita, C. M., & Zagury, G. J. (2018). Determination of point of zero charge of natural organic materials. *Environmental Science and Pollution Research*, *25*, 7823–7833.

Caballero, R.E., Jiménez, V., Miranda, M., Rovira, D., González, P., Ramos-Chue De Pérez, J. Optimización de condiciones para la producción de lacasa por Trametes villosa (Sw.) Kreisel y su aplicación en el biotratamiento de vinazas de caña de azúcar. Anales de Biología, 2021, 43, 27–37.

Caballero, R. E., Jimenez, V., Miranda, M., Rovira, D., Branda, G., & Perez, J. R. C. (2024). An optimal culture medium for laccase production and sugar cane vinasse biotreatment with Trametes villosa using Plackett-Burman and central composite designs. *Applied Environmental Research*, *46*(1), 001.

Caputo, M. (2020). *Estudio de la composicion organica de la vinaza y metodologias para eliminar sus efectos contaminantes* [PhD Thesis]. Universidad Nacional de La Plata.

Cascaret-Carmenaty, D. A., Rodriguez-Matos, J., Ricardo-Lobaina, C. A., Quesada-Gonzalez, O., & Bahin-Deroncele, L. (2020). Utilizacion de bagazo de cana de azucar natural y tratado quimicamente, como material adsorbente para Cu^{2+}. *Revista Cubana de Quimica*, *32*(2), 331–344.

Chakraborty, T. K., Ghosh, S., Islam, M. S., Nice, M. S., Islam, K. R., Netema, B. N., Rahman, Md. S., Habib, A., Zaman, S., Ghosh, G. C., Hossain, Md. R., Tul-Coubra, K., Adhikary, K., Munna, A., Haque, Md., M., Bosu, H., & Halder, M. (2023). Removal of hazardous textile dye from simulated wastewater by municipal organic solid waste charcoal using machine learning approaches: Kinetics, isotherm, and thermodynamics. *Heliyon*, *9*(8), e18856.

Chingono, K. E., Sanganyado, E., Bere, E., & Yalala, B. (2018). Adsorption of sugarcane vinasse effluent on bagasse fly ash: A parametric and kinetic study. *Journal of Environmental Management*, 224, 182–190.

Christofoletti, C. A., Escher, J. P., Correia, J. E., Marinho, J. F. U., & Fontanetti, C. S. (2013). Sugarcane vinasse: Environmental implications of its use. *Waste Management*, *33*, 2752–2761.

Chumpiboon, A., Thongsubsai, K., Pongsiri, T., Knijnenburg, J. T. N., & Ngernyen, Y. (2022) Removal of cationic dye from textile wastewater using treated bagasse fly ash: An industrial waste. *Engineering and Applied Science Research*, *49*(3), 381–394.

Crespão, L. P., Rosenberger, A. G., Lima, F. S., Bertéli, M. B. D., Dragunski, D. C., Colauto, N.B., Linde, G. A., Goncalves, Jr. A. C. & Caetano, J. (2021). Sugarcane biomass colonized by Pleurotus ostreatus for red 4B dye removal: a sustainable alternative. *Environmental Technology*, *42*(17), 2611–2623.

Dai, Y., Sun, Q., Wang, W., Lu, L., Liu, M., Li, J., Yang, S., Sun, Y., Zhang, K., Xu, J., Zheng, H., Yang, Y., Gao, Y., Chen, Y., Zhang, X., Gao, F., & Zhang, Y. (2018). Utilizations of agricultural waste as adsorbent for the removal of contaminants: A review. *Chemosphere*, 211, 235–253.

de Aquino Lima, F., Santos Junior, A. C., Sarrouh, B., & Lofrano, R. C. Z. (2024). Application of sugarcane bagasse and peanut shell in *natura* as bioadsorbents for vinasse treatment. *Clean Technologies and Environmental Policy*, 26, 401–416.

Donaldson, L. (2020). Autofluorescence in plants. *Molecules*, *25*(10), 2393.

Gholizadeh, A., Kermani, M., Gholami, M., & Farzadkia, M. (2013). Kinetic and isotherm studies of adsorption and biosorption processes in the removal of phenolic compounds from aqueous solutions: Comparative study. *Journal of Environmental Health Science and Engineering*, 11, 1–10.

Gomes, M. G., Gurgel, L. V. A., Baffi, M. A., & Pasquini, D. (2020). Pretreatment of sugarcane bagasse using citric acid and its use in enzymatic hydrolysis. *Renewable Energy*, *157*, 332–341.

Hoang, M. T., Pham, T. D., Pham, T. T., Nguyen, M. K., Nu, D. T. T., Nguyen, T.H., Bartling, S., & Van der Bruggen, B. (2021). Esterification of sugarcane bagasse by citric acid for Pb2+ adsorption: Effect of different chemical pretreatment methods. *Environmental Science and Pollution Research*, *28*, 11869–11881.

Hu, Q., Lan, R., He, L., Liu, H., & Pei, X. (2023). A critical review of adsorption isotherm models for aqueous contaminants: Curve characteristics, site energy distribution and common controversies.

Journal of Environmental Management, *329*, 117104.

Hubbe, M., Azizian, S., & Douven, S. (2019). Implications of apparent pseudo-second-order adsorption kinetics onto cellulosic materials: A review. *BioResources*, *14*, 7582–7626.

Inglezakis, V. J., & Zorpas, A. A. (2012). Heat of adsorption, adsorption energy and activation energy in adsorption and ion exchange systems. *Desalination and Water Treatment*, *39*, 149–157.

Jacome-Pilco, C. R., Garcia-Culqui, R. M., Guevara-Narvaez, L. A., & Moreta-Guangasi, T. Y. (2023). Revalorizacion del bagazo de cana de azucar (Saccharum officinarum) como residuo importante para la agroindustria. *593 Digital Publisher CEIT*, *8*(3), 134–148

Jaramillo Gonzalez, N. A. (2025). *Evaluación de la capacidad del bagazo de caña de azúcar (Saccharum officinarum) como bioadsorbente para la remoción de fenoles en vinazas*. [Magister en Investigación Thesis]. Universidad Autónoma de Chiriquí.

Kee, W. C., Wong, Y. S., Ong, S. A., Lutpi, N. A., Sam, S. T., Dahalan, F. A., Chai, A. & Eng, K.M. (2023). Chemical and biological combined treatment for sugarcane vinasse: Selection of parameters and performance studies. *Environmental Science and Pollution Research*, *30*, 65364–65378.

Kerrou, M., Bouslamti, N., Raada, A., Elanssari, A., Mrani, D., & Slimani, M. S. (2021). The use of sugarcane bagasse to remove the organic dyes from wastewater. *International Journal of Analytical Chemistry*, 5570806.

Koopmann, A. K., Schuster, C., Torres-Rodríguez, J., Kain, S., Pertl-Obermeyer, H., Petutschnigg, A., & Hüsing, N. (2020). Tannin-based hybrid materials and their applications: A review. *Molecules*, *25*(21), 4910.

Ly, H. T. Y., Dieu, H. T. K., Sang, T. M. T., & Nha, L. N. M. (2018). Chemically modified sugarcane bagasse as a biosorbent for dye removal from aqueous solution. *Science and Technology Development Journal - Natural Sciences*, *2*(6), 175–181.

Marin, N., Carvajal, R., Chung, A., Perez, A., & Solis, J. Fabricacion y caracterizacion de conductividad termica de materiales aislantes a base de fibras naturales. *Revista de Iniciacion Cientifica*, *7*(1), 67–70.

MICI. (2008). *Reglamento Técnico DGNTI-COPANIT 39-2000 "Agua. Descargas de efluentes líquidos directamente a sistemas de recolección de aguas residuales"* (pp. 1–30). Panamá: Ministerio de Comercio e Industrias.

MICI. (2019). *Reglamento Técnico DGNTI-COPANIT 35-2019 "Medio ambiente y protección de la salud. Seguridad. Calidad del Agua. Descarga de Efluentes líquidos a cuerpos y masas de agua continentales y marinas"* (pp. 1–40). Panamá: Ministerio de Comercio e Industrias.

Miguel-Gallo, Y., Rodríguez Rico, I. L., & Prieto García, J. O. (2017). Influencia del pH y la temperatura en la adsorción de fenol en agua utilizando ceniza de bagazo de caña de azúcar. *Afinidad: Journal of Chemical Engineering Theoretical and Applied Chemistry*, 74, 579.

Ministerio de Desarrollo Agropecuario. Proyeccion de la produccion agricola en Panama, ano agricola 2022-2023. (2023, June 22). *Datos Abiertos de Panama*, 2023. https://www.datosabiertos.gob.pa/dataset/mida-proyeccion-de-la-produccion-agricola-en-panama

Montiel-Rosales, A., Montalvo-Romero, N., Garcia-Santamaria, L. E., Sandoval-Herazo, L. C., Bautista-Santos, H., & Fernandez-Lambert, G. (2022). Post-industrial use of sugarcane ethanol vinasse: A systematic review. *Sustainability*, *14*, 11635.

Mpatani, F. M., Aryee, A. A., Kani, A. N., Wen, K., Dovi, E., Qu, L., Li, Z., & Han, R. (2020). Removal of methylene blue from aqueous medium by citrate modified bagasse: Kinetic, equilibrium and thermodynamic study. *Bioresource Technology Reports*, *11*, 100463.

Mpatani, F. M., Han, R., Aryee, A. A., Kani, A. N., Li, Z., & Qu, L. (2021). Adsorption performance of modified agricultural waste materials for removal of emerging micro-contaminant bisphenol A: A comprehensive review. *Science of the Total Environment*, *780*, 146629.

Nguyen, M. K., Hoang, M. T., Pham, T. T., & van der Bruggen, B. (2019). Performance comparison of chemically modified sugarcane bagasse for removing Cd(II) in water environment. *Journal of Renewable Materials*, *7*, 415–428.

Othmani, A., Magdouli, S., Senthil Kumar, P., Kapoor, A., Chellam, P.V., & Gokkuş, O. (2022). Agricultural waste materials for adsorptive removal of phenols, chromium (VI) and cadmium (II) from wastewater: A review. *Environmental Research*, *204*, 111916.

Papirio, S., Frunzo, L., Mattei, M.R., Ferraro, A., Race, M., D'Acunto, B.,Firozzi, F., & Lens, P. N. L. (2017). Heavy metal removal from wastewaters by biosorption: Mechanisms and modeling. In Rene, E. R., Sahinkaya, E., Lewis, A., & Lens, P. N. L. (Eds.). *Sustainable heavy metal remediation: Volume 1: Principles and processes* (pp. 25–63). Springer International Publishing.

Reis, C. E. R., & Hu, B. (2017). Vinasse from sugarcane ethanol production: Better treatment or better utilization? *Frontiers in Energy Research*, *5*, 7.

Rulli, M. M., Villegas, L. B., Barcia, C. S., & Colin, V. L. (2021). Bioconversion of sugarcane vinasse into fungal biomass protein and its potential use in fish

farming. *Journal of Environmental Chemical Engineering*, *9*, 106136.

Samuel, P. N. K. J., Soosai, M. R., Moorthy, I. G., & Sankar, K. (2020). Material and process selection for biosorption. In Jerold, M., Arockiasamy, S., & Sivasubramanian V. (Eds.), *Bioprocesses engineering for* bioremediation (pp. 241–259). Springer Nature.

Santos, V. C. G., Salvado, A. P. A., Dragunski, D. C., Peraro, D. N. C., Tarley, C. R. T., & Caetano, J. (2012). Highly improved chromium (III) uptake capacity in modified sugarcane bagasse using different chemical treatments. *Quimica Nova*, *35*(8), 1606–1611.

Schönherr, J., Buchheim, J. R., Scholz, P., & Adelhelm, P. (2018). Boehm titration revisited (Part I): Practical aspects for achieving a high precision in quantifying oxygen-containing surface groups on carbon materials. *Journal of Carbon Research*, *4*(2), 21.

Silva, A. F. R., Brasil, Y. L., Koch, K., & Amaral, M. C. S. (2021). Resource recovery from sugarcane vinasse by anaerobic digestion - A review. *Journal of Environmental Management*, *295*, 113137.

Siqueira, T. C. A., Silva, I. Z. da, Rubio, A. J., Bergamasco, R., Gasparotto, F., Paccola, E. A. de S., & Yamaguchi, N. U. (2020). Sugarcane bagasse as an efficient biosorbent for methylene blue removal: Kinetics, isotherms and thermodynamics. *International Journal of Environmental Research and Public Health*, *17*, 526.

Solano, I., Aguilar, O., Dominguez, C., Ramirez, G., & Aguilar, O. (2020). Evaluacion del rendimiento energetico del bagazo de cana de un ingenio azucarero vs su aprovechamiento mediante gasificacion. *Revista de Iniciacion Cientifica*, *6*(1), 30–35.

Soto, M. L., Moure, A., Domínguez, H., & Parajó, J. C. (2011). Recovery, concentration and purification of phenolic compounds by adsorption: A review. *Journal of Food Engineering*, *105*, 1–27.

Torres, E. (2020). Biosorption: A review of the latest advances. *Processes*, *8*, 1584.

Tyagi, U., & Anand, N. (2024). Sustainable and low-cost biomass derived adsorbents for the removal of toxic contaminants from wastewater: Approaches and future perspective. *Waste Management Bulletin*, *2*, 308–325.

Ungureanu, N., Vladuț, V., & Biriș, S. Ș. (2022). Sustainable valorization of waste and by-products from sugarcane processing. *Sustainability*, 14, 27.

Vareda, J. P. (2023). On validity, physical meaning, mechanism insights and regression of adsorption kinetic models. *Journal of Molecular Liquids*, *376*, 121416.

Wang, J., & Guo, X. (2020). Adsorption isotherm models: Classification, physical meaning, application and solving method. *Chemosphere*, *258*, 127279.

Yadav, S., Yadav, A., Bagotia, N., Sharma, A. K., & Kumar, S. (2021). Adsorptive potential of modified plant-based adsorbents for sequestration of dyes and heavy metals from wastewater: A review. *Journal of Water Process Engineering*, *42*, 102148.

Zara, J., Yegres, F., Vargas, N., Morales, S., Cubillan, L., Navas, P., & Marquez-Riquel, M. (2017). Empleo de la espectroscopia infrarroja (FT-IR-ATR) como herramienta para la caracterizacion del bagazo de cana proveniente de la Sierra Falconiana. *Quimica Viva*, *16*(3), 17–24.